Comparative Biochemistry and Physiology - Part D: Genomics and Proteomics 56 (2025) 101575

Contents lists available at ScienceDirect

Comparative Biochemistry and Physiology - Part D: Genomics and Proteomics

journal homepage: www.elsevier.com/locate/cbpd

Research article

Genome-wide identification and characterization of *IGF/IGFR/IGFBP* gene families in spotted sea bass and their expression profiles in response to environmental stress

Chong Zhang [a,1], Xinlin Yang [a,1], Yonghang Zhang [a], Shaosen Yang [b], Cong Liu [a], Pengyu Li [a], Lingyu Wang [a], Xin Qi [a], Kaiqiang Zhang [a], Haishen Wen [a], Yun Li [a,*]

[a] *Key Laboratory of Mariculture, Ministry of Education (KLMME), Ocean University of China, Qingdao 266003, China*
[b] *Agro-Tech Extension Center of Guangdong Province, Guangzhou 510500, China*

ARTICLE INFO

Edited by Chris Martyniuk

Keywords:
IGF signaling system
Gene families
Gene expression
Stress response
Spotted sea bass

ABSTRACT

Insulin-like growth factor (IGF) signaling pathway constitutes an ancient regulatory network essential for neuroendocrine functions, significantly influencing developmental processes, reproductive activities, and adaptation to environmental challenges. In this study, we detected 3 *IGF* genes, 3 *IGFR* genes and 11 *IGFBP* genes in spotted sea bass genome. The annotation accuracy and evolutionary conservation of identified genes were confirmed through phylogenetic, syntenic and copy number analyses. Molecular basis of gene functions, and protein interaction relationships were investigated by gene structure and protein-protein interaction (PPI) network analyses. Moreover, selective pressure analysis revealed that most genes primarily underwent purifying selection during evolution. Furthermore, RNA-Seq datasets were utilized to analyze tissue expression profiling for *IGF/IGFR/IGFBP* genes, along with documentation of their environmental stress-responsive transcriptional dynamics in targeted tissues. Our results demonstrated that *IGF/IGFR/IGFBP* genes were widely expressed in different tissues, with several genes exhibiting high expression levels in specific tissues. Additionally, the stress response mechanisms of IGF signaling system mainly involve IGFs functions regulated by IGFBPs and IGF-independent functions of IGFBPs. Notably, *igf1*, *igf2*, *igfbp1a*, *igfbp3b* and *igfbp4* were pinpointed as key functional genes of environmental challenge adaptation in this species. This investigation provides foundational insights into the *IGF/IGFR/IGFBP* gene families in spotted sea bass, delivering the first comprehensive genomic resource for these gene families while clarifying their functional contributions to environmental stress adaptation.

1. Introduction

The insulin-like growth factor (IGF) signaling system, an ancient regulatory axis crucial for vertebrate neuroendocrine control, governs growth and developmental processes (De Santis and Jerry, 2007; Chandhini et al., 2021). This system primarily comprises insulin-like growth factors (IGFs), insulin-like growth factors receptors (IGFRs) and insulin-like growth factor binding proteins (IGFBPs) (Neirijnck et al., 2019; Chandhini et al., 2021). Pituitary-derived growth hormone (GH) activates tissue-specific receptors to stimulate IGF synthesis, establishing a neuroendocrine regulatory cascade (Bianchi et al., 2017). Mature IGFs are single-stranded polypeptides characterized by evolutionarily conserved gene structures, which could activate multiple intracellular signal transduction pathways by binding to IGFRs in target tissues, thereby initiating specific actions and regulating physiological processes across different tissues (Wood et al., 2005; Gauguin et al., 2008). IGF1R is the primary tyrosine kinase receptor responsible for signal transduction in the IGF pathway, which comprises a ligand-binding domain in the extracellular α subunit and a transmembrane β subunit housing tyrosine kinase activity. The phosphorylation of tyrosine kinase domain, triggered by the binding of ligand-binding domain and IGFs, initiates multiple downstream signal pathways, thereby mediating signal transduction in the IGF signaling pathway (White, 2003; Wood et al., 2005). While IGF2R is a multifunctional glycoprotein

* Corresponding author.
E-mail address: yunli0116@ouc.edu.cn (Y. Li).
[1] These authors contributed equally to this work.

https://doi.org/10.1016/j.cbd.2025.101575
Received 13 April 2025; Received in revised form 20 June 2025; Accepted 2 July 2025
Available online 6 July 2025

present on the cell surface with multi transmembrane structures, the absence of tyrosine kinase region results in the inability of IGF2R to activate the conventional IGFs signal transduction. Instead, it regulates the levels of free ligand by binding and degrading extracellular IGFs (Wood et al., 2005; Nolan et al., 2006). In addition, IGFBPs serve as critical components that could modulate the binding of IGFs to their receptors, thereby either enhancing or inhibiting the activity and function of IGFs (Clemmons, 2016; Allard and Duan, 2018). Their conserved N- and C-terminal domains form high-affinity IGF-binding interfaces, while the central linker region's structural diversity enables IGF-independent functions through interactions with own special receptors (Zhu et al., 2008; Clemmons, 2016; Allard and Duan, 2018).

For aquaculture fishes, IGF signaling system contains three ligand types (*igf1*, *igf2,* and *igf3*), two receptor types (*igf1r* and *igf2r*) and seven types of IGF-binding protein (*igfbp1–7*) (Chandhini et al., 2021; Li et al., 2021). Hepatic tissue serves as the primary synthesis site for *igf1* in fish, though broader tissue distribution occurs via local signaling through paracrine/autocrine mechanisms (Reindl et al., 2011; Fuentes et al., 2013). *Igf2* is also widely expressed in different tissues and displays distinct tissue-specific expression profiles across species: liver and muscle dominance in zebrafish (*Danio rerio*) versus liver and kidney dominance in common carp (*Cyprinus carpio*) (Tse et al., 2002; Rotwein, 2018). The functions of *igf1* and *igf2* have been elucidated in extensive studies, confirming their roles in regulating cell growth through cell metabolism, proliferation and differentiation, thus underscoring their crucial roles in fish growth and development (Caldarone et al., 2016; Chandhini et al., 2021; Khatab et al., 2014; Li et al., 2015a). As a teleost-specific subtype, *igf3* demonstrates gonad-biased expression patterns and plays pivotal roles in oogenesis and spermatogenesis, underscoring its essentiality in fish reproduction (Li et al., 2021). The bioavailability of *igf3* is likely modulated by *IGFBPs*, given the broad transcriptional activity of multiple *IGFBP* genes in ovarian tissue. This regulatory paradigm gains further support from the evolutionarily conserved downregulation of *igfbp3* during final oocyte maturation in zebrafish (Li et al., 2019b) and rainbow trout (*Oncorhynchus mykiss*) (Kamangar et al., 2006).

Apart from functions in regulating growth and reproduction, this signaling network has been investigated for its response to abiotic stress factors including starvation, osmotic pressure, and oxygen limitation, especially for *IGFBPs* which could operate IGF-independent functions (McLellan et al., 1992; Ayson et al., 2007; Link et al., 2010). Starvation studies in Atlantic salmon (*Salmo salar*) revealed coordinated hepatic *igfbp1a* induction and muscular *igf1* suppression, in addition, the differential expression of *igf2* and *igfbp1a/b* in liver were also observed for golden pompano (*Trachinotus ovatus*) under starvation challenges, suggesting their synergistical regulation for growth and metabolism under starvation conditions (Breves et al., 2016; Chen et al., 2024). In freshwater and seawater transition experiments for tilapia, *igf1* and *igf2* genes were upregulated significantly in gills. Complementary evidence from humpback grouper (*Cromileptes altivelis*) demonstrated salinity-responsive expression of *igf1*, *igf2r*, *igfbp1a*, and *igfbp5a* in brain tissue. These collective findings highlight tissue-specific modulation of the IGF signaling system during teleost osmoregulation (Link et al., 2010; Chen et al., 2024). Moreover, previous studies in zebrafish further demonstrate hypoxia-induced upregulation of *igfbp1* in both adults and embryos. Additionally, thermal challenges trigger differential expressions of *igf1/2*, *igfbp1a/b*, *igfbp2b*, and *igfbp5b* for liver tissue of golden pompano. These findings underscore the essential regulatory role of IGFBPs within the IGF signaling system particularly in mediating stress response mechanisms (Maures and Duan, 2002; Kajimura et al., 2006; Allard and Duan, 2018; Chen et al., 2024). Despite these advances, stress-responsive functional mechanisms of IGF signaling remain ambiguities in fish studies, especially regarding the functions of IGFBPs in IGF signaling system responding to stresses (Chandhini et al., 2021). Therefore, understanding the response mechanism of IGF signaling system under environmental stresses holds critical importance for further elucidating the genetic mechanism of fish resistance traits.

As a euryhaline and eurythermic teleost species, Spotted sea bass (*Lateolabrax maculatus*) demonstrates broad ecological plasticity along coastal ecosystems of China (Sun et al., 2021). Renowned for premium flesh quality and nutritional composition (Liu et al., 2020; Wang et al., 2020), spotted sea bass has gained substantial commercial significance and emerged as a promising aquaculture fish species in China. Nevertheless, the industry sustainability of spotted sea bass is threatened by various environmental stresses including fluctuations in salinity and alkalinity, heat stress, hypoxia conditions, resulting in the reduction of quality and yield of fish and severely affecting economic benefits. Therefore, many functional genes associated with stress tolerance including *slc4* (Wang et al., 2020), *nhe* (Liu et al., 2019), *mapk* (Tian et al., 2019), *hsp90*, and *hsp70* (Sun et al., 2021) have been identified and functionally characterized following exposure to environmental stresses. Despite these advancements, the identification of *IGF/IGFR/IGFBP* genes and their regulatory contributions to stress adaptation remain undefined in spotted sea bass. Hence, this investigation employs comprehensive multi-omics mining to systematically identify and characterize *IGF/IGFR/IGFBP* genes in spotted sea bass. Phylogenetic, syntenic, copy number and selective pressure analyses were conducted to confirm their annotation and investigate their evolutionary relationships. Furthermore, the molecular basis of gene functions was explored through gene structure and protein-protein interaction (PPI) network analyses. Additionally, expression profiling of *IGF/IGFR/IGFBP* genes were examined across different tissues under physiological conditions and in specific tissues following exposure to environmental stresses including salinity, alkalinity, heat, and hypoxia. These findings advance the molecular characteristics of *IGF/IGFR/IGFBP* gene families and provide insight into potential functions of IGF signaling system in spotted sea bass for environmental stress response.

2. Materials and methods

2.1. Genome-wide identification of IGF/IGFR/IGFBP genes in spotted sea bass

A comprehensive identification of *IGF/IGFR/IGFBP* gene sequences was performed through cross-species homology alignment against the spotted sea bass reference genome (PRJNA407434) and RNA-Seq datasets (PRJNA347604). Manual curation was implemented through BLASTP verification against NCBI's non-redundant (nr) database to eliminate false positive/negative. Conserved protein sequences from human (*Homo sapiens*), zebrafish (*Danio rerio*), and large yellow croaker (*Larimichthys crocea*) were used as queries in TBLASTN searches with strict similarity thresholds (*E*-value $\leq$1e−5). Open reading frames (ORFs) of candidate genes were predicted using the NCBI ORF Finder tool and validated via BLASTP alignment against the NCBI non-redundant protein database. Protein physicochemical properties, including molecular weight (MW), theoretical isoelectric point (pI), and subcellular localization, were predicted using ProtParam and EukmPLoc 2.0. Genome-wide collinearity analysis was conducted with the MCScanX toolkit to identify conserved syntenic blocks (Wang et al., 2012), while chromosomal localization of *IGF/IGFR/IGFBP* genes was mapped to the reference genome. Gene duplication events and chromosomal distributions were visualized using the amazing super circos program of TBtools v1.082 (Chen et al., 2020a).

2.2. Phylogenetic, syntenic and copy number analyses

Phylogenetic relationships were constructed using deduced amino acid sequences from *L. maculatus IGF/IGFR/IGFBP* genes, along with orthologous sequences from several representative mammals and teleost including human, mouse (*Mus musculus*), chicken (*Gallus gallus*), cow (*Bos taurus*), zebrafish, Nile tilapia (*Oreochromis niloticus*), large yellow croaker, torafugu (*Takifugu rubripes*), Japanese medaka (*Oryzias latipes*),

channel catfish (*Ictalurus punctatus*), European perch (*Perca fluviatilis*) and Atlantic cod (*Gadus morhua*). Phylogenetic trees were generated using MEGA v7.0 with the neighbor-joining (NJ) algorithm under the Jones-Taylor-Thornton (JTT) substitution model, supported by 1000 bootstrap replicates (Kumar et al., 2016). Resultant trees were refined for visualization using the iTOL platform (https://itol.embl.de/). Syntenic conservation was assessed by comparing genomic regions flanking *IGF/IGFR/IGFBP* genes across spotted sea bass, zebrafish, and human genomic data sourced from NCBI database. Additionally, gene copy numbers within these gene families were quantified across L. *maculatus* and other representative vertebrates to delineate duplication patterns.

2.3. Gene structure and domain analysis

Functional domains of spotted sea bass IGF/IGFR/IGFBP proteins were annotated using the SMART 7.0 database (http://smart.embl.de/), and the exon-intron structures were derived from the general feature format (GFF) files of reference genome. Subsequently, the gene structures were visualized using online GSDS 2.0 software (http://gsds.cbi.pku.edu.cn).

2.4. Protein-protein interaction (PPI) network prediction

A protein interaction network for deduced IGF/IGFR/IGFBP amino acid sequences was inferred using STRING 11.0 (https://string-db.org/), employing a zebrafish ortholog based computational framework to model putative interaction landscapes among spotted sea bass IGF system proteins.

2.5. Selective pressure analysis

Coding sequences of *IGF/IGFR/IGFBP* genes from spotted sea bass and several representative vertebrates including human, mouse, chicken, cattle, zebrafish, channel catfish, Atlantic cod, Japanese medaka, Nile tilapia, torafugu, larger yellow croaker and European perch were aligned via ClustalW algorithm (Wang et al., 2020). Phylogenetic trees were generated using Maximum Parsimony (MP) methods in MEGA 7.0 based on the aligned results (Kumar et al., 2016). Evolutionary selection pressures were assessed using branch-site models in the codeml program of PAML software, with MP-derived gene trees as input topology. Spotted sea bass was designated as the foreground lineage, while adequate and representative vertebrate species constituted background branches for comparative analysis(Yang, 2007). The branch-site framework (model = 2, Nsites = 2) tested two scenarios: a neutral model restricting one site category to $\omega = 1$ (fix_omega = 1, omega = 1) and a selection model allowing $\omega > 1$ for codons on foreground branches (fix_omega = 0, omega = 1.5). Initial $\omega = 1.5$ was set to facilitate model convergence following recent teleost genome analyses (Yang, 2007; Yang et al., 2019; Wang et al., 2020). Likelihood ratio tests (LRT) compared model fits, with statistical significance determined by $\chi 2$ distribution analysis of twice the log-likelihood differences (Yang et al., 2019). For significant results (P-value <0.05), the posterior probability of positive selection sites could be calculated by Bayes Empirical Bayes (BEB) method, and the presence of positive selection sites with probability value >0.95 indicates that the gene is under positive selection pressure in evolution (Yang et al., 2005). Spatial localization of these sites on protein secondary structures was visualized using Protter (http://wlab.ethz.ch/protter/start/).

2.6. Expression profiles of IGF/IGFR/IGFBP genes in different tissues by analysis of RNA-Seq datasets

RNA-Seq datasets including gill (SRR7528883), stomach (SRR7528884), liver (SRR7528886), brain (SRR7528887), spleen (SRR752888), testis (SRR7528885) and ovary (SRR2937376) were acquired from NCBI. Raw sequencing data underwent quality filtering with Trimmomatic v0.39 to eliminate adapter sequences and low confidence reads. Subsequently, high-quality clean reads were aligned against the reference genome of spotted sea bass (PRJNA407434) using Hisat2 v2.2.1 software and the mapped reads from alignments were sorted using samtools v1.6 software. Transcript abundance was quantified and normalized to fragments per kilobase of transcript per million fragments mapped (FPKM) by StringTie v2.1.7 software (Bolger et al., 2014; Pertea et al., 2016). Finally, TBtools v1.082 software was used to display heatmap of gene expression levels using $\log_2$(FPKM+1).

2.7. Challenge experiments under various environmental stresses

To investigate the functional roles of IGF signaling system under various environmental stresses, RNA-Seq datasets from prior challenge experiments involving salinity, alkalinity, heat, and hypoxia stresses were analyzed to evaluate expression profiling of *IGF/IGFR/IGFBP* genes. The process of challenge experiments was described briefly as follows:

For salinity challenge experiment, 108 spotted sea bass individuals (body weight: 127.35 ± 15.31 g) were evenly divided into 9 water tanks for salinity acclimation (salinity: 30 ‰) for a week. After that, the salinity of 3 tanks gradually adjusted to 0 ‰ within 12 h, which was set as freshwater group (FW). And the salinity of another 3 tanks gradually adjusted to 12 ‰ within 12 h, which was set as brackish water group (BW). The salinity of the remaining 3 tanks was maintained at 30 ‰, which was set as seawater group (SW). The experiment period lasted for 30 days, during which the other environmental factors remained unchanged. Gill tissues from six individuals per tank were harvested, flash-frozen in liquid nitrogen, and stored at −80 °C for RNA isolation after experiment.

For alkalinity challenge experiment, 45 individuals (body weight: 140.32 ± 2.56 g) were pre-acclimated to freshwater (pH: 7.8 ± 0.4) for 30 days before exposure to alkalinity stress (carbonate alkalinity: 18 ± 0.2 mmol/L, pH 9.0 ± 0.2) in triplicate tanks. Alkaline water was prepared by dissolving $NaHCO_3$ (12.8 mmol/L) and Na_2CO_3 (2.6 mmol/L) in freshwater, followed by 24-h aeration. Gill tissue samples from three fish per tank were collected at 0, 12, 24 and 72 h post-exposure, preserved in liquid nitrogen, and stored at −80 °C.

For high temperature stress test, 60 individuals (body weight: 38.96 ± 2.01 g) were acclimated in a tank for 2 weeks, then distributed into triplicate tanks at 25 °C for 48 h. Then water temperature was ramped at 1 °C/h to 32 °C and maintained. Liver tissues from three fish per tank were sampled at 0, 3, 6, 12, and 24 h post-heat exposure, flash-frozen in liquid nitrogen, and stored at −80 °C.

For hypoxia stress test, 60 individuals (body weight:178.25 ± 18.56 g) were acclimated for two weeks before transfer to triplicate tanks with hypoxic water (dissolved oxygen: 1.1 ± 0.14 mg/L). Dissolved oxygen levels were regulated through a combination of oxygen consumed by fish and air injected. Gill tissues from three fish per tank were collected at 0, 3, 6, and 12 h post-exposure, snap-frozen, and stored at −80 °C for subsequent RNA analysis.

2.8. Expression profiles of IGF/IGFR/IGFBP genes in response to various environmental stresses by analysis of RNA-Seq datasets

Total RNA from stress-challenged tissues was isolated with TRIzol® reagent (Invitrogen, USA), with quality verification via Biodropsis BD-1000 spectrophotometry (OSTC, China) and gel electrophoresis. Three random RNA samples from the same tank were selected to ensure robust biological replication within experimental groups, and these RNA samples were further pooled with equal amounts to create mixed samples. For salinity challenge experiment, 9 sequencing libraries (3 experimental group × 3 replicated samples) were constructed and 150 bp paired-end reads (PRJNA611641) were generated using Illumina Novaseq™ 6000 (PRJNA515986). For the alkalinity challenge experiment, 12 sequencing libraries (4 time points ×3 replicated samples)

were constructed and 150 bp paired-end reads (PRJNA611641) were generated using Illumina HiSeq X Ten sequencing platform. For high temperature challenge experiment, 15 sequencing libraries (5 time points ×3 replicated samples) were constructed and 150 bp paired-end reads (SRR30002608-SRR30002622) were generated using illumina Novaseq™ 6000 sequencing platform. For hypoxia challenge experiment, 12 sequencing libraries (4 time points ×3 replicated samples) were constructed and 150 bp paired-end reads (PRJNA408177) were generated using Illumina HiSeq 4000 sequencing platform.

The FPKM values of *IGF/IGFR/IGFBP* genes in specific tissues after challenge experiment were obtained following the RNA-Seq datasets analysis procedure described in section 2.7. The fold change of differential expressions of each *IGF/IGFR/IGFBP* genes was determined by calculating the FPKM ratios at different time points to that at 0 h. Differential expression significance ($P < 0.05$) was determined via SPSS 25.0, with log2-transformed fold-change values visualized as clustered heatmaps using TBtools v1.082.

3. Results

3.1. Characterizations of IGF/IGFR/IGFBP genes in spotted sea bass

A total of 3 *IGF* genes (*igf1*, *igf2* and *igf3*), 3 *IGFR* genes (*igf1ra*, *igf1rb* and *igf2r*) and 11 *IGFBP* genes (*igfbp1a*, *igfbp1b, igfbp2a, igfbp2b, igfbp3a, igfbp3b, igfbp4, igfbp5a, igfbp5b, igfbp6* and *igfbp7*) were identified in spotted sea bass, and the coding sequences (CDS) of all genes had been submitted to NCBI database. Their detailed information and access numbers were provided in Table 1. The predicted protein lengths ranged from 177 to 215, 1126 to 2104, and 201 to 291 amino acids for *IGF/IGFR/IGFBP* genes, respectively, with considerable variations in molecular weights (MWs) and isoelectric points (pI) across IGF/IGFR/IGFBP proteins. The results of subcellular localization indicated that IGF1Ra and IGF1Rb primarily localize to cell membrane, while the other proteins predominantly reside extracellularly.

Furthermore, *IGF/IGFR/IGFBP* genes of spotted sea bass were dispersed among 11 chromosomes, including chr1, chr3, chr6, chr9, chr10, chr12, chr13, chr16, chr17, chr18 and chr24 (Fig. 1). Notably, certain *IGFBP* genes exhibited adjacent positions on the chromosomes, indicative of potential genomic duplications. For instance, *igfbp1a* and *igfbp3a* genes were neighboring on chromosome 23, along with their paralogous genes *igfbp1b* and *igfbp3b* on chromosome 2. Similar patterns were also observed for *igfbp2* and *igfbp5* genes, with *igfbp2a* and *igfbp5a* genes located adjacently on the chromosome 18, and *igfbp2b* and *igfbp5b* adjacent on the chromosome 13 (Fig. 1). Given the widespread presence of collinear block in whole genome, it is plausible that duplicated *IGFBP* genes of spotted sea bass primarily resulted from the teleost-specific whole genome duplication (WGD) event (Liu et al., 2019; Wang et al., 2020).

3.2. Phylogenetic, copy number and syntenic analyses of IGF/IGFR/IGFBP genes

Phylogenetic analysis revealed *igf1*, *igf2* and *igf3* genes of spotted sea bass were distributed into 3 separate clades and were well clustered with respective counterparts in selected species (Fig. 2A**)**. Of which, *igf1* and *igf3* genes were single copy in selected vertebrates and *igf3* was a teleost specific gene, while *igf2* gene harbored two copies only in a few freshwater fish like channel catfish, zebrafish, and common carp (Fig. 2A**,** Table 2). The phylogenetic tree of *IGFR* genes has two main clades (*igf1r* and *igf2r*) in selected species, of which, the clustering pattern of *igf1r* gene appeared more conserved than *igf2r* gene, suggesting greater sequence divergence among species for *igf2r* gene (Fig. 2B). *Igf1r* harbored two copies in all selected teleost but were single copy in mammals, while *igf2r* was consistently single copy in all selected vertebrates (Fig. 2B**,** Table 2). Furthermore, phylogenetic relationships of *IGFBP* genes indicated the presence of 7 distinct clades, with *IGFBP* genes of spotted sea bass showing close clustering with counterparts from other species (Fig. 2C). The *IGFBP* gene copy numbers in spotted sea bass are largely consistent with most teleost, except for the *igfbp6* gene. This gene exists as a single copy in spotted sea bass but typically appears duplicated in zebrafish and channel catfish. A similar pattern occurs with *igfbp4*, which is absent in zebrafish and channel catfish while present as a single copy in most teleost (Fig. 2C**,** Table 2).

To further confirm the annotation accuracy and explore gene evolutionary relationship, the neighboring genes of *IGF/IGFR/IGFBP* genes in spotted sea bass, zebrafish and human were compared by syntenic analysis. Despite some differences in gene arrangement, neighboring genes of *IGF/IGFR/IGFBP* genes were basically consistent among the three species (Fig. S1). In addition, tandem arrangement events were also observed for *igfbp1/3* and *igfbp2/5* genes in tested three species (Fig. S1C), indicating that conserved genomic neighborhood of *IGF/IGFR/IGFBP* genes. These findings confirm the annotation accuracy of *IGF/IGFR/IGFBP* genes in spotted sea bass and underscore their relatively conserved evolutionary nature.

3.3. Gene structure and domain analysis of IGF/IGFR/IGFBP genes

To delve deeper into the molecular basis of gene functions, gene structure and domain analysis was employed to elucidate the conservatism and diversity of gene structures (Fig. 3). The paralogous *IGF* genes exhibited similar exon-intron structures, with *igf1* and *igf3* genes comprising 4 exons each, while *igf2* gene possessed 5 exons. The core

Table 1
Summary of characteristics of *IGF/IGFR/IGFBP* genes in spotted sea bass.

Gene Name	ORF length (bp)	Amino acid (aa)	Molecular Weight (kDa)	Isoelectric Point (pI)	Subcellular localization	Accession Number
igf1	558	185	20.45	9.63	Extracellular	PQ630847
igf2	648	215	24.60	10.04	Extracellular	PQ630848
igf3	534	177	19.74	9.46	Extracellular	PQ630849
igf1ra	4251	1416	159.69	5.89	Cell membrane	PQ630850
igf1rb	3381	1126	125.00	5.91	Cell membrane	PQ630851
igf2r	6315	2104	230.14	5.58	Extracellular	PQ630852
igfbp1a	792	263	27.98	6.85	Extracellular	PQ630853
igfbp1b	744	247	26.46	5.85	Extracellular	PQ630854
igfbp2a	876	291	32.38	7.39	Extracellular	PQ630855
igfbp2b	807	268	29.81	6.59	Extracellular	PQ630856
igfbp3a	861	286	30.84	9.03	Extracellular	PQ630857
igfbp3b	870	289	31.78	9.07	Extracellular	PQ630858
igfbp4	786	261	28.75	7.43	Extracellular	PQ630859
igfbp5a	813	270	29.83	9.12	Extracellular	PQ630860
igfbp5b	795	264	29.09	8.69	Extracellular	PQ630861
igfbp6	606	201	21.74	8.96	Extracellular	PQ630862
igfbp7	816	271	28.37	6.14	Extracellular	PQ630863

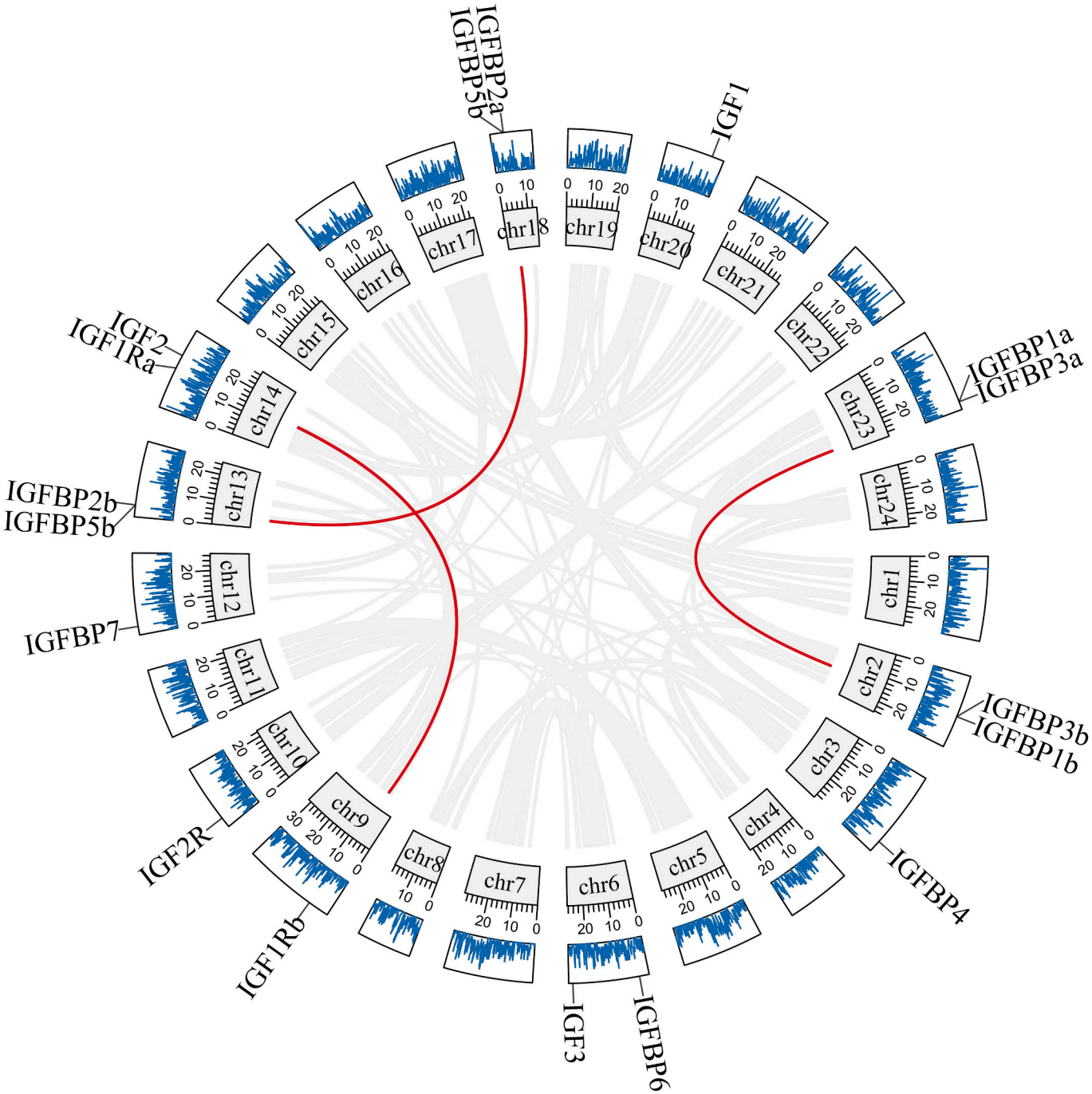

Fig. 1. Chromosome distribution and duplication mode of *IGF/IGFR/IGFBP* genes in spotted sea bass. The gray line represents the whole genome collinear block, and the red line represents the tandem repeat between genes, and the blue outer ring indicates the gene density.

functional domain for all *IGF* genes was identified as IIGF, a family of proteins including insulin, relaxin and IGFs, which corresponds to the B-C-A domain of IGFs (Chandhini et al., 2021; Li et al., 2021), underscoring the relatively conserved nature of gene structure and functional domain for *IGF* genes (Fig. 3A). In contrast, *IGFR* genes displayed notable differences in exon numbers and exon-intron structures. Specifically, the exon numbers of *igf1ra*, *igf1rb* and *igf2r* were 21, 20 and 44 respectively with significant variations of exon-intron structure observed between *IGF1R* and *IGF2R* genes (Fig. 3B). Functional domain analysis revealed distinct features for *IGF1R* and *IGF2R* genes. *IGF1R* genes mainly harbored ligand binding site (Recep_L_domain), furin-like repeats domian (FU), fibronectin Type 3 domain (FN3), Tyrosine kinase, catalytic domain (TyrKc), and transmembrane domain with only 23 amino acids located between FN3 and TyrKc domain (Fig. 3B). Nevertheless, *IGF2R* gene possessed a relatively simple gene structure and functional domain, including signal peptide, fibronectin Type 2 domain (FN2), transmembrane domain and cation-independent mannose-6-phosphate receptor repeat (CIMR) located in the extracellular region (Fig. 3B). Regarding *IGFBP* genes, exon-intron structures were basically consistent, except for *igfbp7*, which comprised 5 exons while *igfbp1–6* all harbored 4 exons. The core functional domain for *IGFBP* genes was insulin growth factor-binding protein homologues (IB), which serve as a high affinity binding partner of IGFs located in the conserved N- terminal region of IGFBPs. In addition, the conserved C- terminal region of *igfbp1–6* genes contained thyroglobulin type I repeats domain (TY), while *igfbp7* gene featured kazal type serine protease inhibitors (KAZAL)

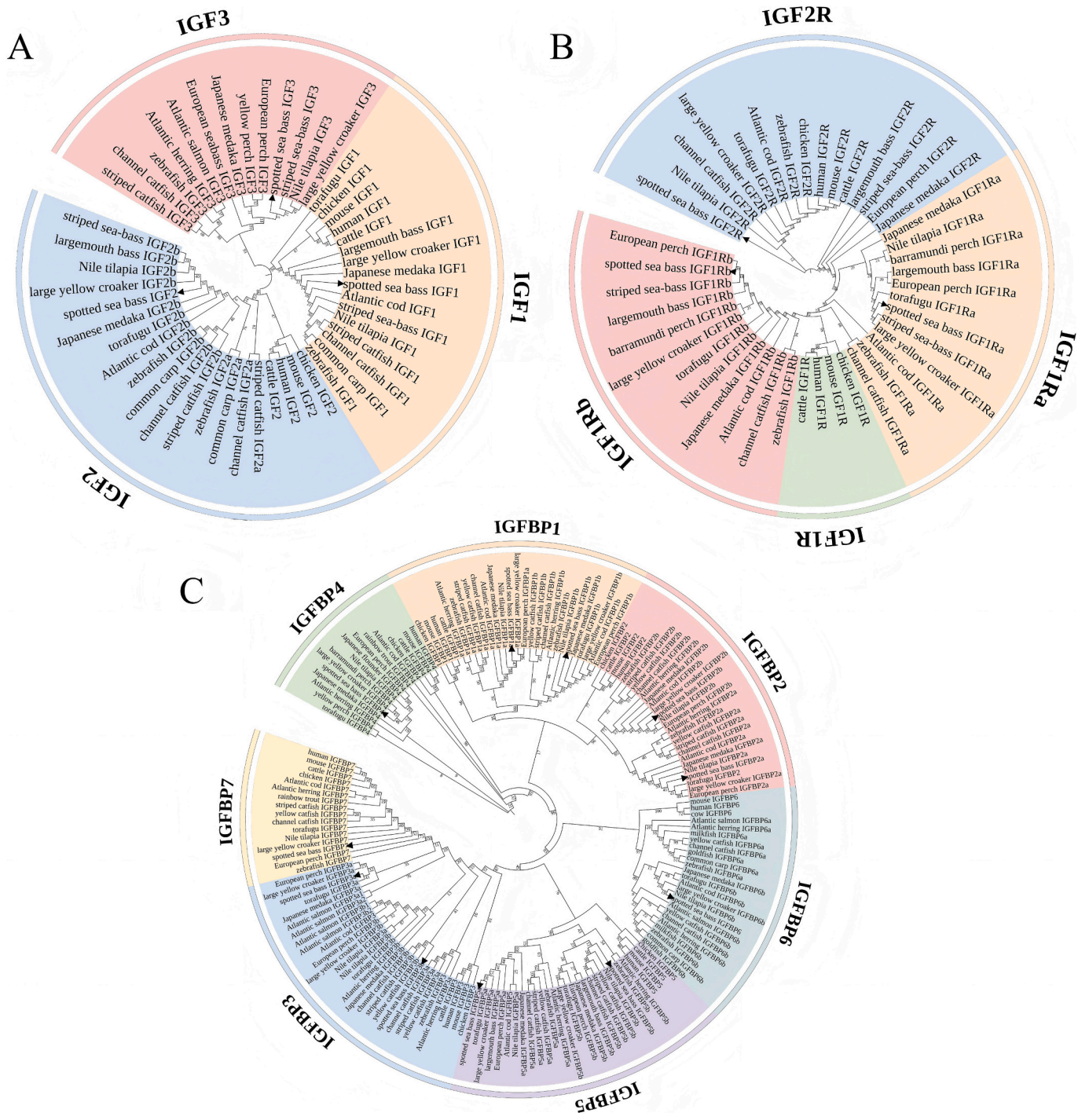

Fig. 2. Phylogenetic relationships of **(A)** *IGF*, **(B)** *IGFR* and **(C)** *IGFBP* gene families among spotted sea bass and selected vertebrate species. The tree was generated with MUSCLE using the neighbor-joining (NJ) method in MEGA 7. Bootstrapping values were indicated by numbers on every node, and the black triangles represent corresponding genes of spotted sea bass.

and immunoglobulin C-2 Type (IGc2) domain instead of TY domain (Fig. 3C).

3.4. Protein-protein interaction network analysis

The PPI network based on zebrafish orthologs displayed interaction relationships of *IGF/IGFR/IGFBP* genes in spotted sea bass (Fig. 4). Notably, IGF1 and IGF2 were found to interact with all IGFRs and IGFBPs, while IGF3 exhibited interactions only with IGF1R and IGFBP3. Furthermore, IGFBPs demonstrated interactions not only with IGFs but also with IGFR and other IGFBPs.

3.5. Selective pressure analysis

Branch-site models including neutral model (model-null) and selection model (model-A) were employed to investigate whether the *IGF/IGFR/IGFBP* genes of spotted sea bass underwent adaptive evolution and LRT tests were used for significance analysis of positive selected sites. The detailed parameter estimates, including models, likelihood value, LRT tests, *p*-values, and positively selected sites with corresponding

Table 2
Analysis of gene copy numbers of *IGF/IGFR/IGFBP* genes in 8 representative vertebrates.

Gene Name	Human	Mouse	Chicken	Zebrafish	Channel catfish	Large yellow croaker	Nile tilapia	Spotted sea bass
igf1	1	1	1	1	1	1	1	1
igf2	1	1	1	2	2	1	1	1
igf3	0	0	0	1	1	1	1	1
igf1r	1	1	1	2	2	2	2	2
igf2r	1	1	1	1	1	1	1	1
igfbp1	1	1	1	2	2	2	2	2
igfbp2	1	1	1	2	2	2	2	2
igfbp3	1	1	1	2	2	2	2	2
igfbp4	1	1	1	0	0	1	1	1
igfbp5	1	1	1	2	2	2	2	2
igfbp6	1	1	0	2	2	1	1	1
igfbp7	1	1	1	1	1	1	1	1

Yellow areas indicate those teleost-specific genes and blue areas represent genes with multiple copies in all selected teleost.

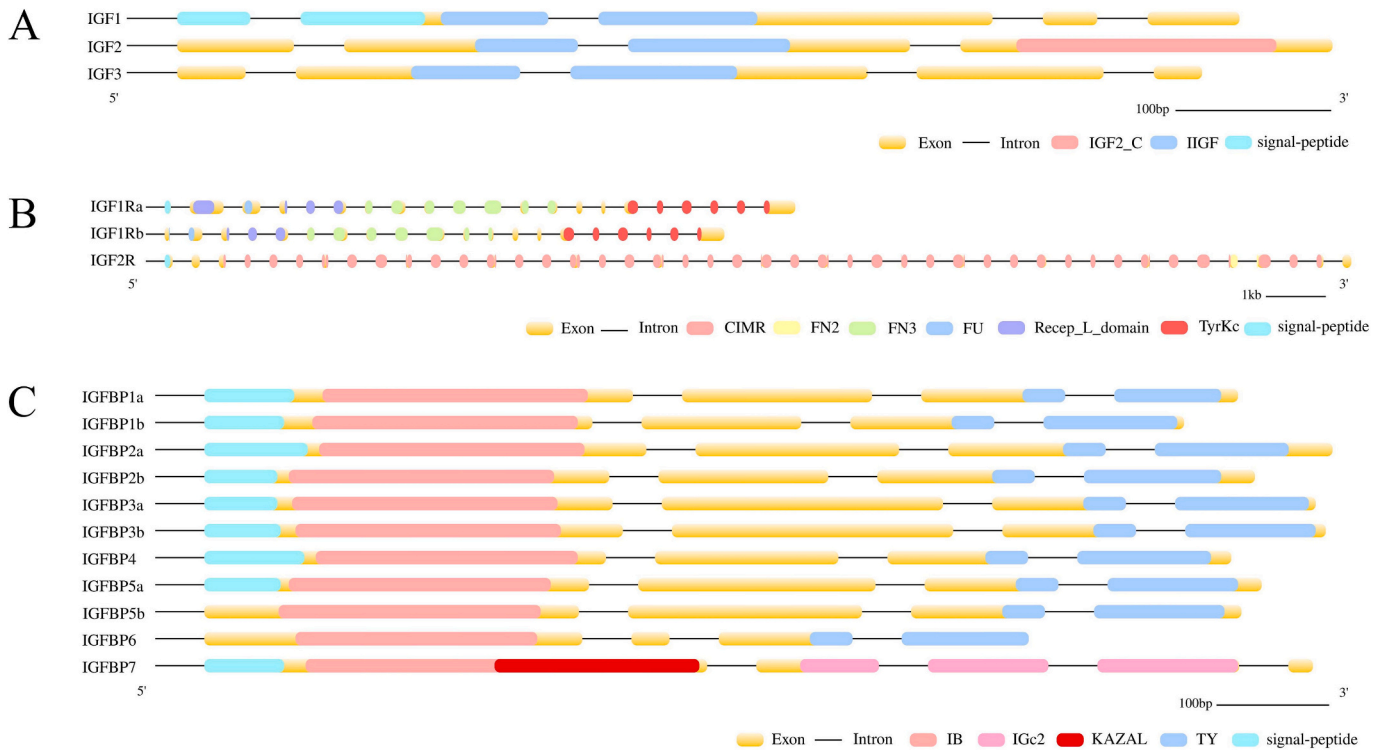

Fig. 3. Schematic representation of gene structures of **(A)** *IGF*, **(B)** *IGFR* and **(C)** *IGFBP* genes for spotted sea bass. The boxes represented exons and lines were intron. The functional domains were marked with different colors.

probability were summarized in Table 3**.** Of which, significant positive selection was detected at 1 site (838S) in *igf1ra* and 5 sites (3C, 23 M, 26 A, 27 T, and 28 T) in *igf1rb*, while no significant positive selection sites were observed in other genes. Noteworthily, although the LRT test supports the credibility of test models, the probability of 1 site (175 N) in *igf2* gene was 0.902, which has not yet reached significant levels in BEB method (Table 3). These results imply that most genes mainly underwent purifying selection during evolution except for *igf1ra* and *igf1rb* genes, suggesting the possibility of functional diversification and adaptation in *igf1ra* and *igf1rb* genes for spotted sea bass. Further examination of predicted secondary structures revealed that 1 positive selection site (838S) of *igf1ra* was located on FN3 domain and 5 positive selection sites of *igf1rb* (3C, 23 M, 26 A, 27 T and 28 T) were located on N-terminal extracellular region (3C and 23 M) and FU domain (26 A, 27 T and 28 T) (Fig. S2).

3.6. Expression profiles of IGF/IGFR/IGFBP genes in different tissues

Using RNA-Seq datasets derived from different tissues of one-year-old spotted sea bass, we preliminarily analyzed the tissue expression profiles of *IGF/IGFR/IGFBP* genes. The results revealed distinct expression patterns across different tissues (Fig. 5**,** Table S1). For *IGF* genes, *igf1* demonstrated liver-specific dominance with limited expression in other tissues. *Igf2* exhibited predominant expressions in the gill, spleen, stomach, and brain, with moderate expression levels. Conversely, *igf2* showed minimal to no expression in the liver, testis, and ovary. *Igf3* displayed lower expression levels in the spleen and testis, with negligible expression detected in other tissues (Fig. 5**,** Table S1). In terms of *IGFR* genes, *igf1ra* was basically not expressed in the stomach and ovary, and *igf1rb* exhibited low expression levels in the liver. Except for this, *IGF1R* and *IGF2R* genes maintained moderate-to-high ubiquitous expression across tissues (Fig. 5**,** Table S1). In addition, the expression patterns of *IGFBP* genes varied considerably among tissues. *Igfbp1a* was highly expressed in all tissues except ovary, *igfbp1b* and *igfbp2b* were highly

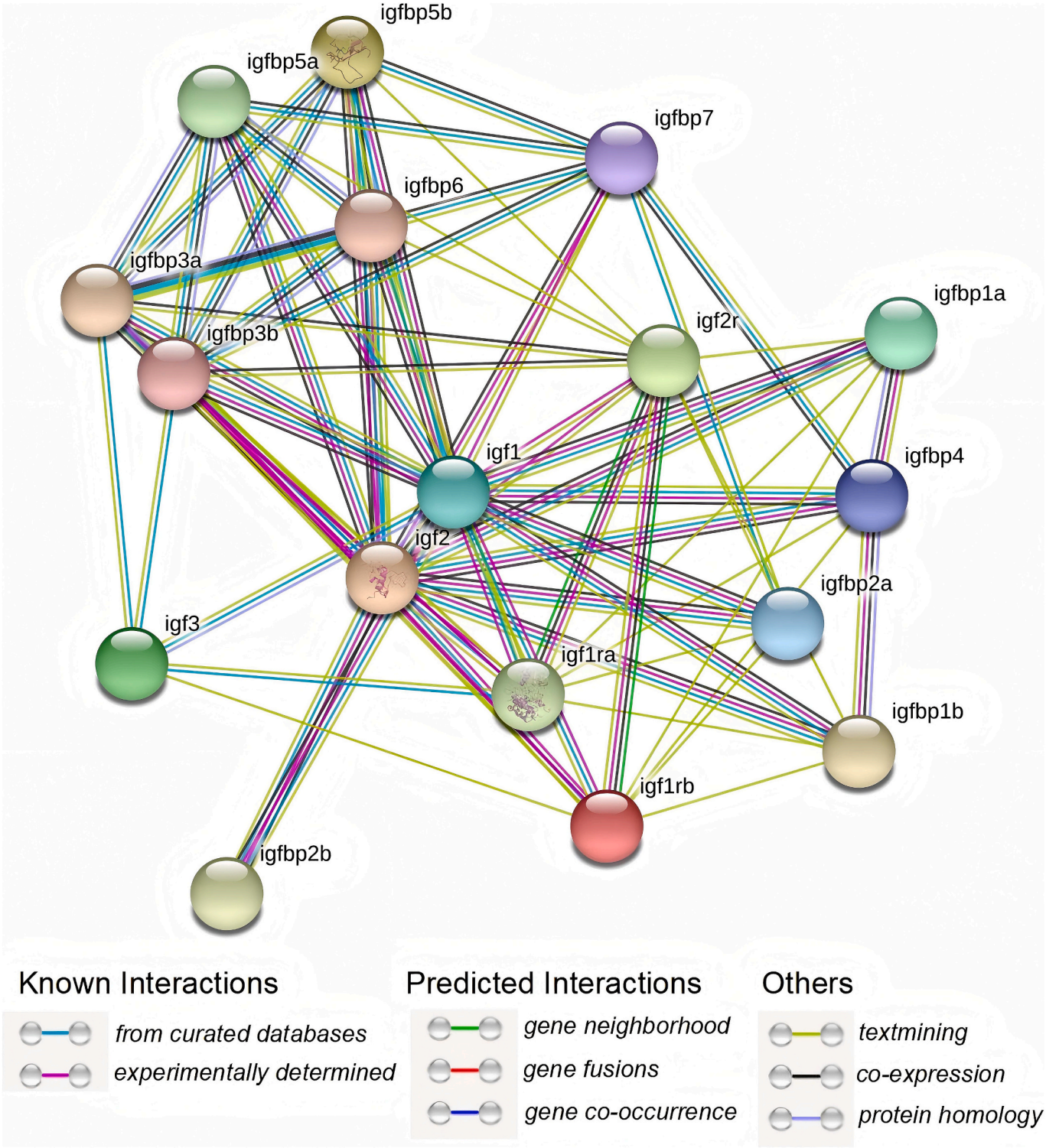

Fig. 4. Putative protein interaction network of *IGF/IGFR/IGFBP* genes in spotted sea bass.

expressed in liver, with minimal or negligible expression in other tissues, and *igfbp2a* was mainly expressed in the brain, liver, and gonads with high or moderate expression levels. *Igfbp3a* and *igfbp3b* displayed main expression sites in the stomach, brain, and testis, albeit with lower expression levels. *Igfbp4* showed significant expression in the gill, stomach, brain, liver, and testis, with the highest expression observed in the gill. *Igfbp5a* predominantly expressed in the gill, spleen and testis, and the expression level in gill was higher than other tissues, while *igfbp5b* exhibited main expression in the spleen, stomach, brain, and testis with lower expression levels. *Igfbp6* showed moderate expression levels in the gill, stomach, brain, and testis with moderate expression levels. Noteworthily, *igfbp7* demonstrated higher expression levels in all tissues, with the highest expression detected in the gill and spleen (Fig. 5, Table S1).

Table 3
The parameters and statistical significances of likelihood ratio tests for the branch-site models.

Gene	Model	np	LnL	Models Compared	2ΔLnL	df	p	Positively Selected Sites
igf1	model-null	25	−1829.70552	MA vs. NMA	0.000	1	1.000e+00	
	model-A	26	−1829.70552					
igf2	model-null	28	−3520.00663	MA vs. NMA	4.73608	1	2.954e-02	175 N 0.902
	model-A	29	-3517.63859					
igf3	model-null	20	−2024.13954	MA vs. NMA	0.000	1	1.000e+00	
	model-A	21	−2024.13954					
igf1ra	model-null	44	−29,524.45821	MA vs. NMA	4.834	1	2.790e-02	838 S 0.973*
	model-A	45	-29,522.04105					
igf1rb	model-null	45	−29,493.85286	MA vs. NMA	40.457	1	2.010e-10	3C 0.998**
	model-A	46	−29,473.62418					23 M 1.000**
								26 A 0.998**
								27 T 0.998**
								28 T 0.998**
igf2r	model-null	27	−43,432.956796	MA vs. NMA	0.000	1	1.000e+00	
	model-A	28	−43,432.956794					
igfbp1a	model-null	40	−7344.369297	MA vs. NMA	0.003	1	9.549e-01	
	model-A	41	−7344.370878					
igfbp1b	model-null	40	−7344.370878	MA vs. NMA	0.000	1	1.000e+00	
	model-A	41	−7344.370878					
igfbp2a	model-null	41	−6680.207086	MA vs. NMA	0.000	1	1.000e+00	
	model-A	42	−6680.207086					
igfbp2b	model-null	41	−6680.168719	MA vs. NMA	0.077	1	7.818e-01	
	model-A	42	−6680.207086					
igfbp3a	model-null	40	−11,353.695599	MA vs. NMA	0.088	1	7.667e-01	
	model-A	41	−11,353.651563					
igfbp3b	model-null	40	−10,707.117981	MA vs. NMA	0.000	1	1.000e+00	
	model-A	41	−11,353.666304					
igfbp4	model-null	25	−4160.35926	MA vs. NMA	0.000	1	1.000e+00	
	model-A	26	−4160.35926					
igfbp5a	model-null	45	−5110.514493	MA vs. NMA	0.000	1	1.000e+00	
	model-A	46	−5110.514500					
igfbp5b	model-null	45	−5109.507461	MA vs. NMA	0.000	1	1.000e+00	
	model-A	46	−5109.507461					
igfbp6	model-null	29	−3106.13067	MA vs. NMA	0.000	1	1.000e+00	
	model-A	30	−3106.13067					
igfbp7	model-null	27	−6300.34636	MA vs. NMA	0.000	1	1.000e+00	
	model-A	28	−6300.34636					

LnL: The natural logarithm of the likelihood value; np: number of parameters; 2LnL: twice the difference in LnL between the two test models compared; sites inferred to be under positive selection at the 95 % level are labeled with single asterisk (*) and those at the 99 % level are labeled with two asterisks (**).

3.7. Expression profiles of IGF/IGFR/IGFBP genes in response to salinity, alkalinity, heat, and hypoxia stress

In the gill tissue following salinity stress (Fig. 6A), the expression levels of *igf1* and *igf2r* at SW group were significantly increased to 1.55- and 2.62- fold in comparison to the FW group. Moreover, *igfbp4* and *igfbp5a* exhibited significant modulated activity with fold change values ranging from 0.69 to 1.33 compared to the FW group (Table S2). In the gill tissue after alkalinity stress (Fig. 6B), there were 7 genes exhibited upregulated expression profile with dynamic time-dependent expression pattern, and the number of upregulated expression genes increased as the alkalinity challenge time was prolonged. Of which, the expression of *igfbp5a* was significantly increased at three points, while the expression of *igfbp7* was significantly increased at 24 h and 72 h. On the other hand, the expressions of *igf2*, *igf1rb*, *igf2r* and *igfbp4* were significantly elevated only at 72 h. Notwithstanding, the fold change values of expression levels of *igf2*, *igf1rb* and *igfbp4* at 72 h were more than double in comparison with 0 h (Table S3). Conversely, only *igfbp1a* expression was significantly decreased at 12 h and 24 h after alkalinity challenge. Following heat stress, gene expression in the liver also exhibited a dynamic time-dependent expression pattern (Fig. 6C). There were 3 genes (*igfbp1a, igfbp1b* and *igfbp3b*) that showed significantly upregulated expression profile, thereinto, the fold change values of expression levels of *igfbp1b* and *igfbp3b* at 24 h had reached >2- and 3-fold compared to 0 h. Notably, highly heat stress-induced expressions in the liver were discovered for *igfbp1a* gene, with expression levels at 6 h, 12 h and 24 h surpassing 4, 13 and 8-fold, respectively, compared to 0 h (Table S4). Additionally, the expression levels of *igfbp2a*, *igfbp2b*, *igfbp3a* and *igfbp6* showed decreased tendency with increasing exposure time to heat stress. In the gill tissue after hypoxia stress (Fig. 6D), the expression levels of 7 genes (*igf2*, *igf1ra*, *igf1rb*, *igf2r*, *igfbp1a*, *igfbp4* and *igfbp7*) were significantly increased with different levels of fold change values (1.39 to 9.63). Of which, *igfbp1a* and *igfbp4* exhibited particularly large fold change values, exceeding 9- and 4-fold, respectively, compared to 0 h (Table S5).

4. Discussion

The IGF signaling pathway, comprising IGFs, IGFRs and IGFBPs, serves as a critical regulatory axis in teleost neuroendocrine systems, orchestrating growth, development, reproductive processes, and stress adaptation (Kajimura et al., 2006; Link et al., 2010; Baroiller et al., 2014; Chandhini et al., 2021). Despite its established roles across fish species, the molecular architecture and functional contributions of *IGF/IGFR/IGFBP* genes remain poorly characterized in spotted sea bass. Addressing this knowledge gap, our study provides the first systematic identification and annotation of these gene families in this species, complemented by transcriptomic profiling under environmental stresses.

Our study identified 3 *IGF* genes (*igf1*, *igf2* and *igf3*), 3 *IGFR* genes (*igf1ra*, *igf1rb* and *igf2r*) and 11 *IGFBP* genes (*igfbp1a*, *igfbp1b, igfbp2a, igfbp2b, igfbp3a, igfbp3b, igfbp4, igfbp5a, igfbp5b, igfbp6* and *igfbp7*) for spotted sea bass from genomic and transcriptomic databases. Phylogenetic analysis revealed 3, 2 and 7 clades for *IGF/IGFR/IGFBP* gene families, with overall better clustering observed for *IGF* and *IGFBP* genes compared to *IGFR* genes, especially for *IGF2R* genes in the absence of

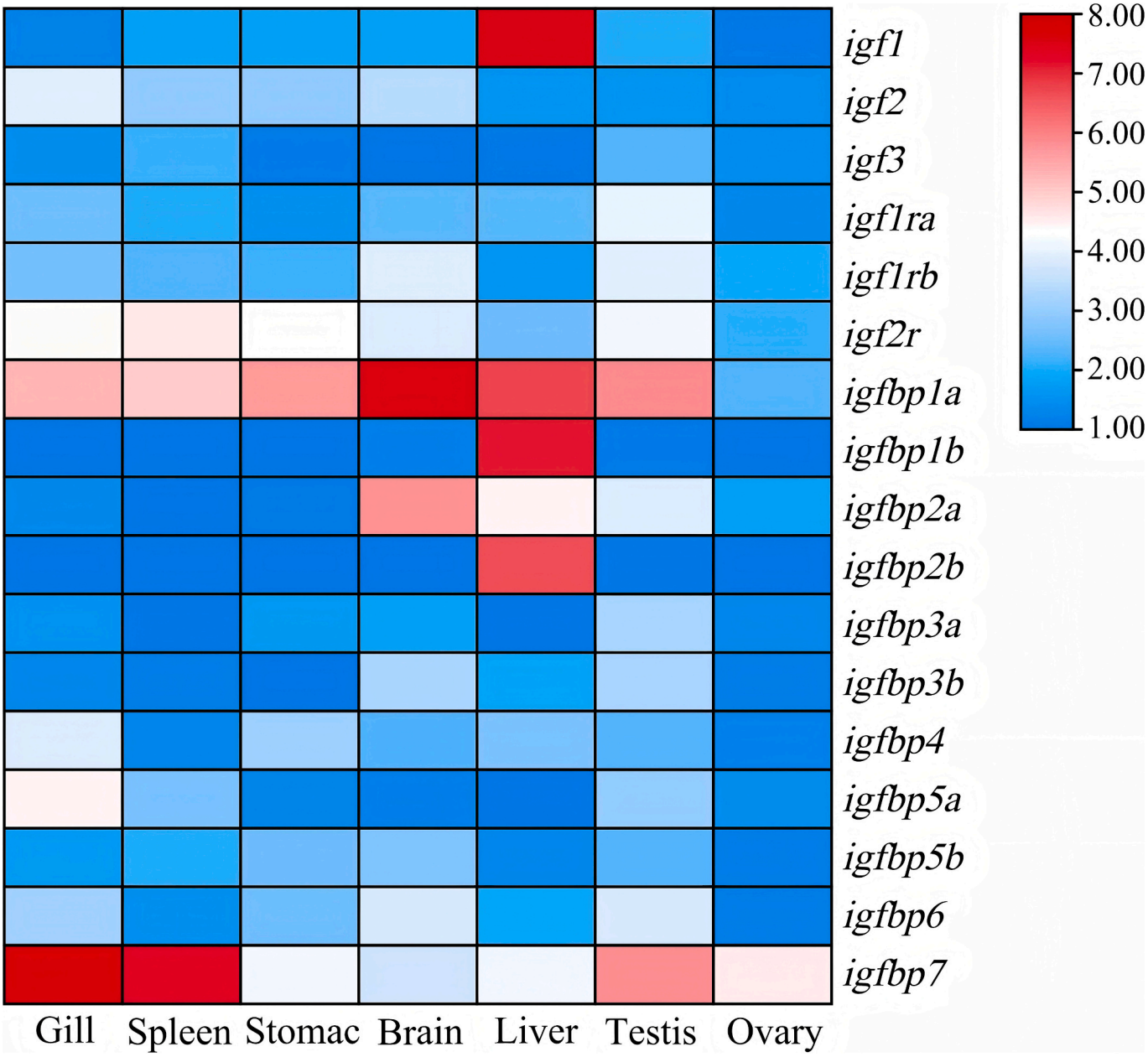

Fig. 5. Expression profiles of *IGF/IGFR/IGFBP* genes in gill, stomach, liver, brain, spleen, and testis tissues for one male spotted sea bass and ovary tissue for one female spotted sea bass based on RNA-Seq datasets. The heatmap is based on $\log_2$(FPKM+1) values.

strong bootstrap values (Fig. 2), suggesting greater sequence divergence among species for *IGFR* genes. Notwithstanding, combined with results of syntenic analysis, the overall similar conditions of neighbor genes between spotted sea bass, human and zebrafish (Fig. S1), corroborating annotation accuracy and evolutionary conservation of identified genes. In addition, the expansion and contraction of *IGF/IGFR/IGFBP* genes were also investigated by gene copy number analysis (Sun et al., 2021). In comparison with *igf1*, *igf2r* and *igfbp7* genes that have identical copy number (single copy) in all vertebrates, there were distinct differences in copy number of other genes between higher vertebrates and teleost (Table 2). Of which, *igf3* was teleost specific gene with single copy, *igf2* gene harbored two copies (*igf2a* and *igf2b*) in a few freshwater fish like channel catfish, zebrafish, and common carp, while only single copy (*igf2b*) was found in most teleost and high vertebrates. Notably, the absence of *igfbp4* gene and copy number doubling of *igfbp6* gene were detected in these freshwater fish (Fig. 2, Table 2), suggesting that the copy number difference of these genes may be resulted from unique gene expansion and contraction during the evolution of these freshwater fish (Li et al., 2015b; Fan et al., 2019). In addition, the copy number of *igf1r*, *igfbp1*, *igfbp2*, *igfbp3* and *igfbp5* genes were doubled in teleost in comparison with high vertebrates. Interestingly, the duplicated subtypes of these genes were distributed among different chromosomes, with *igfbp1* versus *igfbp*3 genes and *igfbp2* versus *igfbp*5 genes being tandemly arranged in the same chromosome (Table 2, Fig. S1). These findings consistently indicated the retention of duplicated genes following teleost-specific whole-genome duplication (WGD) events (Meyer and Van de Peer, 2005; Glasauer and Neuhauss, 2014; Sun et al., 2021).

All *IGF* genes exhibited a relatively simple structure, characterized by a conserved functional domain IIGF (Fig. 3A), which corresponds to the B-C-A functional regions. The B domain, critical for mediating interactions between IGF ligands and IGF1R/IGFBPs (Gauguin et al., 2008; Chandhini et al., 2021), facilitates ligand engagement with the α-subunit's Recep_L domain of IGF1R. This binding triggers tyrosine kinase activation in the β-subunit (Fig. 3B), thereby activating multiple

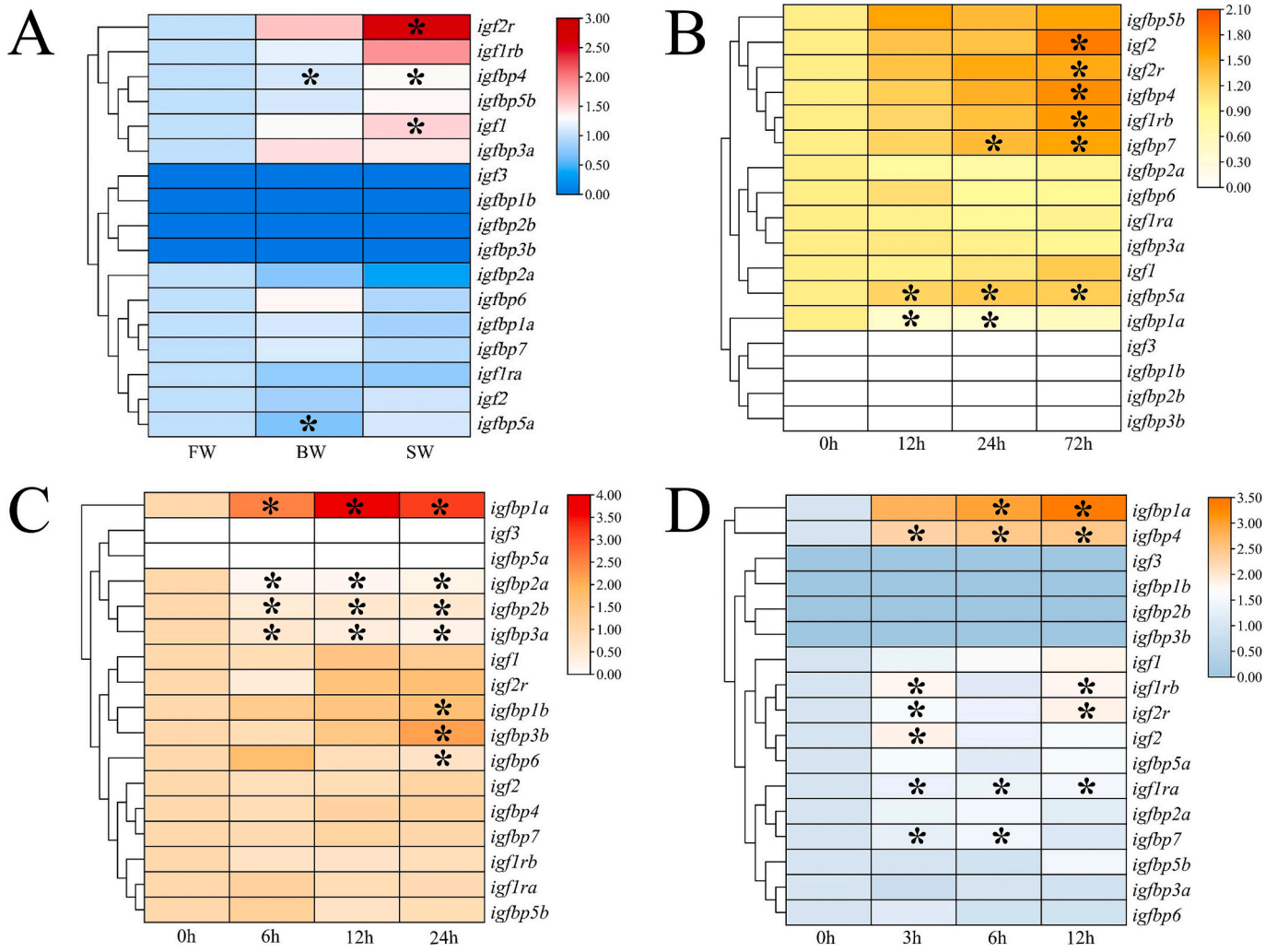

Fig. 6. Expression profiles of *IGF/IGFR/IGFBP* genes of spotted sea bass under different environmental stress based on RNA-Seq datasets. The heatmap is based on $\log_2$(FPKM) values for specific tissues with three replicated samples after challenge experiment. Asterisk (*) indicated the significant differences (*P*-value <0.05). **(A)** Expression profiles of gill under salinity stress. **(B)** Expression profiles of gill under alkalinity stress. **(C)** Expression profiles of liver under heat stress. **(D)** Expression profiles of gill under hypoxia stress.

intracellular signal transduction processes including MAPK-P13 tyrosine kinase pathway and Raf-Mek-Erk1/2 cascade (Pozios et al., 2001; White, 2003; Wood et al., 2005), which ultimately could regulate cell proliferation, survival, and apoptosis (Pollak et al., 2004; Solomon-Zemler et al., 2017). In contrast, the absence of Recep_L_domain in IGF2R prevents the activation of conventional IGFs signal transduction (Fig. 3B). Instead, IGF2R could regulate the levels of free ligands by binding and degrading extracellular IGFs (Wood et al., 2005). However, the molecular identity and function of IGF2R still remain unclear in fishes, necessitating further research concentrated on its detailed function mechanism. In addition, as main component regulating IGFs activity in the IGF signaling pathway, IGFBPs could bind IGFs via high-affinity IGF binding site composited of IB domain located in the N- terminal and TY domain located in the C- terminal (Fig. 3C), thereby altering the equilibrium between the IGFs and IGF1R (Clemmons, 2016; Chandhini et al., 2021). In comparison to the highly conserved N- terminal and C- terminal in IGFBP1–6, the C- terminal of IGFBP7 is no longer conserved, which is also observed in gene structure that IGFBP7 harbored two specific domains (KAZAL and IGc2 domain) instead of TY domain in IGFBP1–6 (Li et al., 2012; Clemmons, 2016) (Fig. 3C). Therefore, the binding ability of IGFBP7 to IGFs was reduced to varying degrees, suggesting the special biological functions of IGFBP7 compared to other IGFBPs (Yamanaka et al., 1997; Li et al., 2012). Moreover, no function domains were detected in the mid-region of N- and C-terminal domain, indicating sequence divergence in linker region among IGFBPs family members, these results also explain why IGFBPs have distinct properties and IGF-independent functions (Clemmons, 2016; Allard and Duan, 2018). Furthermore, stress-responsive expression profiling revealed distinct functional specialization among IGFBP paralogs. For example, only *igfbp5a* exhibited significant downregulated expression profile in response to salinity stress with *igfbp5b* remaining unaltered. For alkalinity stress, only *igfbp1a* and *igfbp5a* showed significantly differential expression pattern while no *igfbp1b* and *igfbp5b*. For heat stress, *igfbp1a* and *igfbp1b* both showed significantly upregulated expression profile, while only *igfbp1a* expression exhibited modulated activity under hypoxia stress. This paralogs-specific partitioning of stress responses likely stems from evolutionary divergence within the central linker regions-structural domains governing functional diversification through post-translational modifications and interaction interfaces. The PPI network further supports this viewpoint, showing interactions where IGFs interact with IGFRs and IGFBPs, while IGFBPs also interact with IGFRs and other IGFBPs except for their interaction with IGFs (Fig. 4), indicating that IGFBPs could perform corresponding biological function independently of IGFs.

Furthermore, to delve deeper into the evolutionary patterns of *IGF/IGFR/IGFBP* genes in spotted sea bass, we employed positive selection

analysis through branch-site models. The result revealed that only 1 and 5 sites within the *igf1ra* and *igf1rb* genes, respectively, exhibited significant evidence of positive selection (Table 3). These data reinforce the evolutionary conservation of the IGF signaling system, as most studied genes appeared constrained by purifying selection, a common evolutionary mechanism preserving protein functionality through selective elimination of deleterious mutations (Sironi et al., 2015). Notably, positive selection sites were exclusively identified in *igf1r* paralogs and spatially confined to extracellular regions harboring FN3 or FU functional domains. Critically, these domains flank the known ligand-binding domain (Recep_L-domain) of IGF1R. This spatial distribution suggests potential adaptive modifications in extracellular molecular interactions, particularly relevant given the established role of the N-terminal extracellular region in ligand binding (Matsunami and Buck, 1997). Mechanistically, the FN3 domain forms the β-sheet scaffold of the IGF-binding core, where it's conserved the F-G loop (FG-loop) directly engages IGF1. The identified substitutions may enhance hydrogen bonding networks and modulate conformational dynamics during ligand binding. Similarly, the FU domain contains a conserved dimerization motif whose hydrophobic core stability governs receptor activation kinetics (Li et al., 2019a). We therefore postulate that positive selection sites may modulate IGF binding affinity and receptor dimerization efficiency. Nevertheless, empirical validation of these molecular mechanisms remains beyond the current scope and warrants future investigation.

Tissue expression profiles of *IGF/IGFR/IGFBP* genes indicate predominantly ubiquitous expressions in various tissues, with varying degrees of expression levels ranging from low to moderate, while certain genes exhibit notably high expression levels in specific tissues. For example, *igf1*, *igfbp1b* and *igfbp2b* genes exhibited marked transcriptional abundance in the liver, indicating that liver is the prime organ for the expression of these three genes (Reindl et al., 2011). Multiple genes including *igf2*, *igf2r*, *igfbp1a*, *igfbp4*, *igfbp5a* and *igfbp7* demonstrate relatively elevated expression levels in gills, suggesting the potential importance of IGF signaling pathway in biological functions of gills for spotted sea bass. Notably, *igf2r*, *igfbp1a* and *igfbp7* were highly expressed in most tissues, reflecting the essential roles these genes play in mediating basic biological functions for most tissues (Li et al., 2012; Chandhini et al., 2021). A striking exception was observed for *igf3*, which displayed minimal expression in the testis and ovary (Fig. 5). This discrepancy might stem from the use of RNA-Seq data derived from juvenile (one-year-old) fish prior to sexual maturation, as *igf3* expression is known to correlate with gonad maturity in teleost (Wang et al., 2008; Li et al., 2021). As spotted sea bass typically reaches sexual maturity at 3-year-old, the expectedly low gonadal *igf3* expression in 1-year-old juveniles aligns with delayed reproductive development in this species.

Transcriptional analysis of spotted sea bass gills exposed to salinity and alkalinity challenges revealed dynamic expression changes in multiple stress-responsive genes (Fig. 6A, Fig. 6B). Notably, transcriptional upregulation of *igf1* under salinity stress and *igf2* under alkaline conditions suggests their specialized roles in gill osmoregulation. The pivotal role of IGFs (specifically referring to IGF1 and IGF2, same below) in fish osmoregulation has been extensively documented in numerous studies including tilapia, Atlantic salmon and humpback grouper, with mechanisms including GH modulation, chloride cell proliferation, suppression of β-cell ion uptake, and enhanced Na^+/K^+ ATPase activity in chloride cells of gills (McCormick et al., 1991; Sakamoto et al., 1997; Xu et al., 1997). Moreover, *igfbp4* was significantly upregulated in the gill under both salinity and alkalinity stresses, whereas *igfbp5a* exhibited a opposite expression profile under salinity and alkalinity stresses. Additionally, *igfbp1a* and *igfbp7* also exhibited opposite expression profile under alkalinity stress (Fig. 6A, Fig. 6B), indicating that the IGFBPs family could be widely involved in responding to osmotic stress, albeit with distinct responding mechanisms. Consistent with our results, in salinity change for juvenile chum salmon (*Oncorhynchus keta*) and smoltification for the Atlantic salmon, the expression levels of *igfbp1*, *igfbp4* and *igfbp5* were also significantly changed in the liver or gill (Taniyama et al., 2016; Breves et al., 2016b). Apart from interaction with IGFs to mediate osmoregulation, there were researches indicating that IGFBPs could independently participate in osmoregulation by restoring disruptive cellular homeostasis to its normal condition under osmotic stress (Berishvili et al., 2006; Taniyama et al., 2016; Chandhini et al., 2021), these results may explain the different expression profiles of *IGFBPs* in response to osmotic stress. We hypothesize that *IGFBPs* with upregulated expression could independently participate in osmoregulation or enhance IGFs effects by concentrating on IGFs locally, thereby increasing IGFs availability for binding to IGF1Rs. Conversely, downregulated expression of *IGFBPs* preventing IGFs from binding to receptors may release more circulating IGFs to mediate osmoregulation (McCormick et al., 1991; Duan and Xu, 2005; Allard and Duan, 2018). Collectively, these findings highlight the vital role of IGF pathway in gill osmoregulation, mediated through functional coordination between IGFs (*igf1*, *igf2*) and IGFBPs (*igfbp4*), with their expression dynamics reflecting adaptive responses to environmental salinity and alkalinity.

Similar situations were also observed in heat and hypoxia stresses, transcriptional responses of multiple *IGFBPs* gene showed distinct regulatory patterns, while only *igf2* gene exhibited a significant upregulation at 3 h after hypoxia stress (Fig. 6C, Fig. 6D), indicating that IGFBPs dominate in the organism's response to heat and hypoxia stresses compared to IGFs. Notably, *igfbp1a* exhibited significantly highly expression pattern in both the liver and gill (Fig. 6C, Fig. 6D), aligning with its established role as a metabolic modulator that the expression level of *igfbp1* is highly induced by starvation, hypoxia, and other stresses. Moreover, the differential expression of *igfbp1a/b* were also observed for golden pompano under starvation challenges or heat challenges, and the upregulation of *igfbp1* in both adults and embryos for zebrafish were detected under hypoxia stress. Higher amounts of IGFBP1 could bind to IGFs and inhibit their activity, thereby reducing development and growth rate and maintaining cellular metabolism at a lower level (Maures and Duan, 2002; Kajimura et al., 2006; Allard and Duan, 2018). These results further support this perspective and consider *igfbp1a* a vital gene in the response to heat and hypoxia stresses for spotted sea bass. Meanwhile, we also detected the expression level of *igfbp3b* was significantly increased under heat stress (Fig. 6C). Although the detailed functional mechanism of IGFBP3 responding to environmental stress has not been well demonstrated, its function of inhibiting cell growth and proliferation has been verified in several studies (Martin et al., 1995; Yamada and Lee, 2009; Chen et al., 2020a, 2020b). In addition, IGFBP3 is the most abundant IGFBP in circulation and the affinity with IGFs is higher than that of IGFs to their receptor (Chen et al., 2020a, 2020b). Therefore, we speculate that the main function mechanism of IGFBP3b involved in stress response is to inhibit IGFs activity, like IGFBP1a. Moreover, the expression level of *igfbp4* in the gill was significantly upregulated under hypoxia stress, as observed previously under salinity and alkalinity stresses (Fig. 6). Given its relatively higher expression level in the gill compared to other tissues (Fig. 5), we consider that *igfbp4* may be a crucial functional gene in response to environmental stress in the gill of spotted sea bass. The rough responding mechanism of IGFBP4 may involve regulated effects on IGFs and IGF-independent actions, which has been well proved in research about mammals (Conover et al., 2004; Ning et al., 2008; Zhu et al., 2008). However, the detailed function mechanism of IGFBP4, as well as the entire IGF signaling system, in response to environmental stresses for aquatic fishes, remain unresolved. We acknowledge that our hypothesis that IGFBPs modulate IGF activity or act independently under stress was inferred from references and multi-omics results rather than experimental validation. We recognize that this knowledge gap underscores the need for mechanistic studies of IGF signaling system in environmental stress response through experimental validation.

5. Conclusion

This study provides the first comprehensive genomic investigation of *IGF/IGFR/IGFBP* gene families in spotted sea bass, identifying 3 *IGF*, 3 *IGFR*, and 11 *IGFBP* genes. Phylogenetic, syntenic, and copy number analyses validated their evolutionary conservation and annotation accuracy, while gene structure and protein interaction network analyses elucidated their molecular architecture and functional interplay. Selective pressure analysis detected localized positive selection at 1 site in *igf1ra* and 5 sites in *igf1rb*, though purifying selection dominated across most loci, underscoring the evolutionary stability of this signaling system. Furthermore, tissue-specific expression profiling revealed ubiquitous transcriptional activity of these genes, emphasizing their roles in fundamental physiological processes. Stress-response transcriptomics further demonstrated the IGF system's critical involvement in environmental adaptation, with *igf1*, *igf2*, *igfbp1a*, *igfbp3b*, and *igfbp4* emerging as key functional genes in coping with abiotic stress. Overall, these findings establish a foundational framework for understanding of *IGF/IGFR/IGFBP* gene families and offer preliminary evidence on the biological roles of the IGF signaling system in environmental stress response.

Supplementary data to this article can be found online at https://doi.org/10.1016/j.cbd.2025.101575.

CRediT authorship contribution statement

Chong Zhang: Writing – original draft, Software, Methodology, Conceptualization. **Xinlin Yang:** Visualization, Software, Methodology. **Yonghang Zhang:** Visualization, Software. **Shaosen Yang:** Resources, Funding acquisition, Conceptualization. **Cong Liu:** Visualization, Software. **Pengyu Li:** Visualization, Software. **Lingyu Wang:** Visualization, Software. **Xin Qi:** Resources, Conceptualization. **Kaiqiang Zhang:** Resources, Methodology. **Haishen Wen:** Resources, Funding acquisition, Conceptualization. **Yun Li:** Writing – review & editing, Methodology, Funding acquisition, Conceptualization.

Declaration of competing interest

The authors declare that they have no competing interests.

Acknowledgments

This research was funded by the Fundamental Research Funds for the Central Universities [grant number: 202461043], National Key Research and Development Program of China [grant number: 2022YFD2400503], and China Agriculture Research System (CARS for Marine Fish Culture Industry) [grant number: CARS-47].

Data availability

Data will be made available on request.

References

Allard, J.B., Duan, C., 2018. IGF-binding proteins: why do they exist and why are there so many? Front. Endocrinol. 9, 117. https://doi.org/10.3389/fendo.2018.00117.

Ayson, F.G., de Jesus-Ayson, E.G.T., Takemura, A., 2007. mRNA expression patterns for GH, PRL, SL, IGF-I and IGF-II during altered feeding status in rabbitfish. *Siganus guttatus*. General and Comparative Endocrinology. 150, 196–204. https://doi.org/10.1016/j.ygcen.2006.08.001.

Baroiller, J.-F., D'Cotta, H., Shved, N., Berishvili, G., Toguyeni, A., Fostier, A., Eppler, E., Reinecke, M., 2014. Oestrogen and insulin-like growth factors during the reproduction and growth of the tilapia *Oreochromis niloticus* and their interactions. Gen. Comp. Endocrinol. 205, 142–150. https://doi.org/10.1016/j.ygcen.2014.07.011.

Berishvili, G., Shved, N., Eppler, E., Clota, F., Baroiller, J.-F., Reinecke, M., 2006. Organ-specific expression of IGF-I during early development of bony fish as revealed in the tilapia, *Oreochromis niloticus*, by in situ hybridization and immunohistochemistry: indication for the particular importance of local IGF-I. Cell Tissue Res. 325, 287–301. https://doi.org/10.1007/s00441-005-0133-9.

Bianchi, V.E., Locatelli, V., Rizzi, L., 2017. Neurotrophic and neuroregenerative effects of GH/IGF1. Int. J. Mol. Sci. 18, 2441. https://doi.org/10.3390/ijms18112441.

Bolger, A.M., Lohse, M., Usadel, B., 2014. Trimmomatic: a flexible trimmer for Illumina sequence data. Bioinformatics 30, 2114–2120. https://doi.org/10.1093/bioinformatics/btu170.

Breves, J.P., Campbell, B., Björnsson, B.T., 2016. Hepatic insulin-like growth-factor binding protein (igfbp) responses to food restriction in Atlantic salmon smolts. Gen. Comp. Endocrinol. 233, 79–87. https://doi.org/10.1016/j.ygcen.2016.05.015.

Breves, J.P., Inokuchi, M., Yamaguchi, Y., Seale, A.P., Hunt, B.L., Watanabe, S., Lerner, D.T., Kaneko, T., Grau, E.G., 2016b. Hormonal regulation of aquaporin 3: opposing actions of prolactin and cortisol in tilapia gill. J. Endocrinol. 230, 325–337. https://doi.org/10.1530/joe-16-0162.

Caldarone, E., MacLean, S., Beckman, B., 2016. Evaluation of nucleic acids and plasma IGF1 levels for estimating short-term responses of postsmolt Atlantic salmon (*Salmo salar*) to food availability. Fish. Bull. 114, 288–301. https://doi.org/10.7755/FB.114.3.3.

Chandhini, s., Trumboo, B., Jose, S., Varghese, T., Manchi, R., Rejish Kumar, V.J., 2021. Insulin-like growth factor signalling and its significance as a biomarker in fish and shellfish research. Fish Physiol. Biochem. 47, 1011–1031. https://doi.org/10.1007/s10695-021-00961-6.

Chen, C., Chen, H., Zhang, Y., Thomas, H.R., Frank, M.H., He, Y., Xia, R., 2020a. TBtools: an integrative toolkit developed for interactive analyses of big biological data. Mol. Plant 13 (8), 1194–1202. https://doi.org/10.1016/j.molp.2020.06.009.

Chen, J., Zhou, T., Lu, W., Zhu, Q., Li, J., Cheng, J., 2024. Comparative survey of coordinated regulation of hypothalamic–pituitary–somatotropic axis in golden pompano (*Trachinotus ovatus*) and humpback grouper (*Cromileptes altivelis*). Comparative Biochemistry and Physiology Part D: Genomics and Proteomics. 49, 101170. https://doi.org/10.1016/j.cbd.2023.101170.

Chen, Y., Zhou, Y., Yang, X., Cao, Z., Chen, X., Qin, Q., Liu, C., Sun, Y., 2020b. Insulin-like growth factor binding protein 3 gene of golden pompano (TroIGFBP3) promotes antimicrobial immune defense. Fish Shellfish Immunol. 103, 47–57. https://doi.org/10.1016/j.fsi.2020.04.002.

Clemmons, D.R., 2016. Role of IGF binding proteins in regulating metabolism. Trends Endocrinol. Metab. 27, 375–391. https://doi.org/10.1016/j.tem.2016.03.019.

Conover, C.A., Bale, L.K., Overgaard, M.T., Johnstone, E.W., Laursen, U.H., Füchtbauer, E.-M., Oxvig, C., van Deursen, J., 2004. Metalloproteinase pregnancy-associated plasma protein a is a critical growth regulatory factor during fetal development. Development 131, 1187–1194. https://doi.org/10.1242/dev.00997.

De Santis, C., Jerry, D., 2007. Candidate growth genes in finfish — where should we be looking? Aquaculture 272, 22–38. https://doi.org/10.1016/j.aquaculture.2007.08.036.

Duan, C., Xu, Q., 2005. Roles of insulin-like growth factor (IGF) binding proteins in regulating IGF actions. Gen. Comp. Endocrinol. 142, 44–52. https://doi.org/10.1016/j.ygcen.2004.12.022.

Fan, H., Zhou, Y., Wen, H., Zhang, X., Zhang, K., Qi, X., Xu, P., Li, Y., 2019. Genome-wide identification and characterization of glucose transporter (glut) genes in spotted sea bass (*Lateolabrax maculatus*) and their regulated hepatic expression during short-term starvation. Comparative Biochemistry and Physiology Part D: Genomics and Proteomics. 30, 217–229. https://doi.org/10.1016/j.cbd.2019.03.007.

Fuentes, E.N., Valdés, J.A., Molina, A., Björnsson, B.T., 2013. Regulation of skeletal muscle growth in fish by the growth hormone – insulin-like growth factor system. Gen. Comp. Endocrinol. 192, 136–148. https://doi.org/10.1016/j.ygcen.2013.06.009.

Gauguin, L., Delaine, C., Alvino, C.L., McNeil, K.A., Wallace, J.C., Forbes, B.E., De Meyts, P., 2008. Alanine scanning of a putative receptor binding surface of insulin-like growth factor-I*. J. Biol. Chem. 283, 20821–20829. https://doi.org/10.1074/jbc.M802620200.

Glasauer, S., Neuhauss, S., 2014. Whole-genome duplication in teleost fishes and its evolutionary consequences. Molecular Genetics and Genomics: MGG. 289, 1045–1060. https://doi.org/10.1007/s00438-014-0889-2.

Kajimura, S., Aida, K., Duan, Fau -, C., Duan, C., 2006. Understanding hypoxia-induced gene expression in early development: in vitro and in vivo analysis of hypoxia-inducible factor 1-regulated zebra fish insulin-like growth factor binding protein 1 gene expression. Mol. Cell. Biol. 26 (3), 1142–1155. https://doi.org/10.1128/MCB.26.3.1142-1155.2006.

Kamangar, B.B., Gabillard, J.-C., Bobe, J., 2006. Insulin-like growth factor-binding protein (IGFBP)-1, −2, −3, −4, −5, and −6 and IGFBP-related protein 1 during rainbow trout Postvitellogenesis and oocyte maturation: molecular characterization, expression profiles, and hormonal regulation. Endocrinology 147, 2399–2410. https://doi.org/10.1210/en.2005-1570.

Khatab, S.A., Hemeda, S.A., El-Nahas, A.F., Abd El Naby, W.S.H., 2014. Genetic polymorphism in IGF-II gene and its relationship with growth rate in Tilapia nilotica. Alexandria Journal of Veterinary Sciences. 43, 26–32. https://doi.org/10.5455/ajvs.167827.

Kumar, S., Stecher, G., Tamura, K., 2016. MEGA7: molecular evolutionary genetics analysis version 7.0 for bigger datasets. Mol. Biol. Evol. 33, 1870–1874. https://doi.org/10.1093/molbev/msw054.

Li, F., Bai, H., Xiong, Y., Fu, H., Jiang, S., Jiang, F., Jin, S., Sun, S., Qiao, H., Zhang, W., 2015a. Molecular characterization of insulin-like androgenic gland hormone-binding protein gene from the oriental river prawn Macrobrachium nipponense and investigation of its transcriptional relationship with the insulin-like androgenic gland hormone gene. Gen. Comp. Endocrinol. 216, 152–160. https://doi.org/10.1016/j.ygcen.2014.12.007.

Li, J., Choi, E., Yu, H., Bai, X.-c., 2019a. Structural basis of the activation of type 1 insulin-like growth factor receptor. Nat. Commun. 10, 4567. https://doi.org/10.1038/s41467-019-12564-0.

Li, J., Wang, Y., Kang, T., Li, X., Niu, C., 2019b. Insulin-like growth factor binding proteins inhibit oocyte maturation of zebrafish. Gen. Comp. Endocrinol. 281, 83–90. https://doi.org/10.1016/j.ygcen.2019.06.002.

Li, J., Liu, Z., Kang, T., Li, M., Wang, D., Cheng, C.H.K., 2021. Igf3: a novel player in fish reproduction†. Biol. Reprod. 104 (6), 1194–1204. https://doi.org/10.1093/biolre/ioab042.

Li, N., Zhang, Z., Zhang, L., Wang, S., Zou, Z., Wang, G., Wang, Y., 2012. Insulin-like growth factor binding protein 7, a member of insulin-like growth factor signal pathway, involved in immune response of small abalone *Haliotis diversicolor*. Fish Shellfish Immunol. 33, 229–242. https://doi.org/10.1016/j.fsi.2012.04.016.

Li, Y., Liu, S., Qin, Z., Yao, J., Jiang, C., Song, L., Dunham, R., Liu, Z., 2015b. The serpin superfamily in channel catfish: identification, phylogenetic analysis and expression profiling in mucosal tissues after bacterial infections. Developmental & Comparative Immunology. 49, 267–277. https://doi.org/10.1016/j.dci.2014.12.006.

Link, K., Berishvili, G., Shved, N., D'Cotta, H., Baroiller, J.-F., Reinecke, M., Eppler, E., 2010. Seawater and freshwater challenges affect the insulin-like growth factors IGF-I and IGF-II in liver and osmoregulatory organs of the tilapia. Mol. Cell. Endocrinol. 327, 40–46. https://doi.org/10.1016/j.mce.2010.05.011.

Liu, Y., Ma, D., Sun, Y., Niu, J., Fan, Y., 2019. Genome-wide identification of the Na^+/H^+ exchanger gene family in *Lateolabrax maculatus* and its involvement in salinity regulation. Comparative Biochemistry and Physiology Part D: Genomics and Proteomics. 29, 286–298. https://doi.org/10.1016/j.cbd.2019.01.001.

Liu, Y., Wang, H., Wen, H., Shi, Y., Zhang, M., Qi, X., Zhang, K., Gong, Q., Li, J., He, F., Hu, Y., Li, Y., 2020. First high-density linkage map and QTL fine mapping for growth-related traits of spotted sea bass (*Lateolabrax maculatus*). Mar. Biotechnol. 22, 526–538. https://doi.org/10.1007/s10126-020-09973-4.

Martin, J.L., Coverley, J.A., Pattison, S.T., Baxter, R.C., 1995. Insulin-like growth factor-binding protein-3 production by MCF-7 breast cancer cells: stimulation by retinoic acid and cyclic adenosine monophosphate and differential effects of estradiol. Endocrinology 136, 1219–1226. https://doi.org/10.1210/endo.136.3.7532580.

Matsunami, H., Buck, L.B., 1997. A multigene family encoding a diverse array of putative pheromone receptors in mammals. Cell 90, 775–784. https://doi.org/10.1016/s0092-8674(00)80537-1.

Maures, T.J., Duan, C., 2002. Structure, developmental expression, and physiological regulation of zebrafish IGF binding protein-1. Endocrinology 143, 2722–2731. https://doi.org/10.1210/endo.143.7.8905.

McCormick, S.D., Sakamoto, T., Hasegawa, S., Hirano, T., 1991. Osmoregulatory actions of insulin-like growth factor-I in rainbow trout (*Oncorhynchus mykiss*). J. Endocrinol. 130, 87–92. https://doi.org/10.1677/joe.0.1300087.

McLellan, K.C., Hooper, S.B., Bocking, A.D., Delhanty, P.J., Phillips, I.D., Hill, D.J., Han, V.K., 1992. Prolonged hypoxia induced by the reduction of maternal uterine blood flow alters insulin-like growth factor-binding protein-1 (IGFBP-1) and IGFBP-2 gene expression in the ovine fetus. Endocrinology 131, 1619–1628. https://doi.org/10.1210/endo.131.4.1382958.

Meyer, A., Van de Peer, Y., 2005. Meyer, A. & Van de Peer, Y. From 2R to 3R: evidence for a fish-specific genome duplication (FSGD). Bioessays 27, 937–945. https://doi.org/10.1002/bies.20293.

Neirijnck, Y., Papaioannou, Nef, S., 2019. The insulin/IGF system in mammalian sexual development and reproduction. Int. J. Mol. Sci. 20, 4440. https://doi.org/10.3390/ijms20184440.

Ning, Y., Schuller, A.G.P., Conover, C.A., Pintar, J.E., 2008. Insulin-like growth factor (IGF) binding protein-4 is both a positive and negative regulator of IGF activity in vivo. Mol. Endocrinol. 22, 1213–1225. https://doi.org/10.1210/me.2007-0536.

Nolan, C.M., McCarthy, K., Eivers, E., Jirtle, R.L., Byrnes, L., 2006. Mannose 6-phosphate receptors in an ancient vertebrate, zebrafish. Dev. Genes Evol. 216, 144–151. https://doi.org/10.1007/s00427-005-0046-3.

Pertea, M., Kim, D., Pertea, G.M., Leek, J.T., Salzberg, S.L., 2016. Transcript-level expression analysis of RNA-seq experiments with HISAT. StringTie and Ballgown. Nature Protocols. 11, 1650–1667. https://doi.org/10.1038/nprot.2016.095.

Pollak, M.N., Schernhammer, E.S., Hankinson, S.E., 2004. Insulin-like growth factors and neoplasia. Nat. Rev. Cancer 4, 505–518. https://doi.org/10.1038/nrc1387.

Pozios, K., Ding, J., Degger, B., Upton, Z., Duan, C., 2001. IGFs stimulate zebrafish cell proliferation by activating MAP kinase and PI3-kinase-signaling pathways. Am. J. Physiol. Regul. Integr. Comp. Physiol. 280, R1230. https://doi.org/10.1152/ajpregu.2001.280.4.R1230.

Reindl, K.M., Kittilson, J.D., Bergan, H.E., Sheridan, M.A., 2011. Growth hormone-stimulated insulin-like growth factor-1 expression in rainbow trout (*Oncorhynchus mykiss*) hepatocytes is mediated by ERK, PI3K-AKT, and JAK-STAT. Am. J. Physiol. Regul. Integr. Comp. Physiol. 301, R236–R243. https://doi.org/10.1152/ajpregu.00414.2010.

Rotwein, P.A.-O., 2018. The insulin-like growth factor 2 gene and locus in nonmammalian vertebrates: organizational simplicity with duplication but limited divergence in fish. J. Biol. Chem. 293 (41), 15912–15932. https://doi.org/10.1074/jbc.RA118.004861.

Sakamoto, T., Shepherd, B.S., Madsen, S.S., Nishioka, R.S., Siharath, K., Richman, N.H., Bern, H.A., Grau, E.G., 1997. Osmoregulatory actions of growth hormone and prolactin in an advanced teleost. Gen. Comp. Endocrinol. 106, 95–101. https://doi.org/10.1006/gcen.1996.6854.

Sironi, M., Cagliani, R., Forni, D., Clerici, M., 2015. Evolutionary insights into host–pathogen interactions from mammalian sequence data. Nat. Rev. Genet. 16, 224–236. https://doi.org/10.1038/nrg3905.

Solomon-Zemler, R., Sarfstein, R., Werner, H., 2017. Nuclear insulin-like growth factor-1 receptor (IGF1R) displays proliferative and regulatory activities in non-malignant cells. PLoS One 12, e0185164. https://doi.org/10.1371/journal.pone.0185164.

Sun, Y., Wen, H., Tian, Y., Mao, X., Li, X., Li, J., Hu, Y., Liu, Y., Li, J., Li, Y., 2021. HSP90 and HSP70 families in *Lateolabrax maculatus*: genome-wide identification, molecular characterization, and expression profiles in response to various environmental stressors. Front. Physiol. 12, 784803. https://doi.org/10.3389/fphys.2021.784803.

Taniyama, N., Kaneko, N., Inatani, Y., Miyakoshi, Y., Shimizu, M., 2016. Effects of seawater transfer and fasting on the endocrine and biochemical growth indices in juvenile chum salmon (*Oncorhynchus keta*). Gen. Comp. Endocrinol. 236, 146–156. https://doi.org/10.1016/j.ygcen.2016.07.020.

Tian, Y., Wen, H., Qi, X., Zhang, X., Li, Y., 2019. Identification of mapk gene family in *Lateolabrax maculatus* and their expression profiles in response to hypoxia and salinity challenges. Gene 684, 20–29. https://doi.org/10.1016/j.gene.2018.10.033.

Tse, M.C.L., Yuen, B.H.Y., Chan, K.M., 2002. PCR-cloning and gene expression studies in common carp (*Cyprinus carpio*) insulin-like growth factor-II. Biochim. Biophys. Acta 1575, 63–74. https://doi.org/10.1016/S0167-4781(02)00244-0.

Wang, D.-S., Jiao, B., Hu, C., Huang, X., Cheng, C.H.K., 2008. Discovery of a gonad-specific IGF subtype in teleost. Biochem. Biophys. Res. Commun. 367, 336–341. https://doi.org/10.1016/j.bbrc.2007.12.136.

Wang, L.-Y., Niu, J., Fan, Y., Liu, Y., 2020. Slc4 gene family in spotted sea bass (*Lateolabrax maculatus*): structure, evolution, and expression profiling in response to alkalinity stress and salinity changes. Genes 11, 1271. https://doi.org/10.3390/genes11111271.

Wang, Y., Tang, H., Debarry, J.D., Tan, X., Li, J., Wang, X., Lee, T.-H., Jin, H., Marler, B., Guo, H., Kissinger, J.C., Paterson, A.H., 2012. MCScanX: a toolkit for detection and evolutionary analysis of gene synteny and collinearity. Nucleic Acids Res. 40, e49. https://doi.org/10.1093/nar/gkr1293.

White, M.F., 2003. Insulin signaling in health and disease. Science 302, 1710–1711. https://doi.org/10.1126/science.1092952.

Wood, A., Duan, C., Bern, H., 2005. Insulin-like growth factor signaling in fish. Int. Rev. Cytol. 243, 215. https://doi.org/10.1016/S0074-7696(05)43004-1.

Xu, B., Miao, H., Zhang, P., Li, D., 1997. Osmoregulatory actions of growth hormone in juvenile tilapia (*Oreochromis niloticus*). Fish Physiol. Biochem. 17, 295–301. https://doi.org/10.1023/A:1007750022878.

Yamada, P.M., Lee, K.-W., 2009. Perspectives in mammalian IGFBP-3 biology: local vs. systemic action. Am. J. Phys. Cell Phys. 296, C954–C976. https://doi.org/10.1152/ajpcell.00598.2008.

Yamanaka, Y., Wilson, E.M., Rosenfeld, R.G., Oh, Y., 1997. Inhibition of insulin receptor activation by insulin-like growth factor binding proteins. J. Biol. Chem. 272, 30729–30734. https://doi.org/10.1074/jbc.272.49.30729.

Yang, L., Jiang, H., Wang, Y., Lei, Y., Chen, J., Sun, N., Lv, W., Wang, C., Near, T.J., He, S., 2019. Expansion of vomeronasal receptor genes (OlfC) in the evolution of fright reaction in ostariophysan fishes. Communications Biology. 2, 235. https://doi.org/10.1038/s42003-019-0479-2.

Yang, Z., 2007. Yang ZH.. PAML 4: phylogenetic analysis by maximum likelihood. Mol. Biol. Evol. 24, 1586–1591. https://doi.org/10.1093/molbev/msm088.

Yang, Z., Wong, W., Nielsen, R., 2005. Bayes empirical bayes inference of amino acid sites under positive selection. Mol. Biol. Evol. 22, 1107–1118. https://doi.org/10.1093/molbev/msi097.

Zhu, W., Shiojima, I., Ito, Y., Li, Z., Ikeda, H., Yoshida, M., Naito, A.T., Nishi, J.-i., Ueno, H., Umezawa, A., Minamino, T., Nagai, T., Kikuchi, A., Asashima, M., Komuro, I., 2008. IGFBP-4 is an inhibitor of canonical Wnt signalling required for cardiogenesis. Nature 454, 345–349. https://doi.org/10.1038/nature07027.